Geometric Control and Differential Flatness of a Quadrotor UAV with Load Suspended from a Pulley

Jun Zeng, Prasanth Kotaru and Koushil Sreenath

***Abstract*— We study a quadrotor with a cable-suspended load, where the cable length can be controlled by applying a torque on a pulley attached to the quadrotor. A coordinate-free dynamical model of the quadrotor-pulley-load system with nine degrees-of-freedom and four degrees-of-underactuation is obtained by taking variations on manifolds. Under the assumption that the radius of the pulley is much smaller than the length of cable, the quadrotor-pulley-load system is established to be a differentially-flat system with the load position, the quadrotor yaw angle and the cable length serving as the flat outputs. A nonlinear geometric controller is developed, that enables tracking of outputs defined by either (a) quadrotor attitude, (b) load attitude, (c) load position and cable length. Specifically, the design of the controllers for load position and cable length are taken into consideration as a whole unit due to the dynamical coupling of the quadrotor-pulley-load system. Stability proofs for the control design in each case and a simulation of the proposed controller to navigate through a sequence of windows of varying sizes is presented.**

I. Introduction

A wide range of applications of unmanned aerial vehicles (UAVs), such as quadrotors, hexacopters and octocopters, have been used to transport external loads in the recent years. To accomplish a reliable and efficient transportation using small UAVs, researchers have applied various methods in design, path planning, and control. One such method is, where the payload is attached to the aerial robot through a gripper arm [7]. Such a mechanism provides more degrees-of-freedom (DOFs) to the UAV system and increases the number of control inputs as well. However, carrying an external load through a gripper increases the inertia of the system and results in the quadrotor having a sluggish attitude response, making it less robust to perturbations.

An alternative method is to carry a payload suspended through a cable. Early work has focussed on minimization of swing-free maneuvers and trajectory generation to meet various aerial manipulation objectives [8]. Control design for the suspended-load using a single quadrotor was studied in [9], [11], [13]. Dynamics and planning for a payload suspended through cables from multiple quadrotors was carried out in [10], while the control design was carried out in [6], [14]. Recently, control of a quadrotor with load suspended through an elastic cable was studied in [4].

While all previous work regarded the cable length as invariant or indirectly changeable due to the elasticity in the cable, we are motivated by the consideration: what if the cable length can be purposely altered by a mechanism, such as a pulley. This quadrotor-pulley-load system not only adds an additional DOF but also introduces additional challenges:

- A variable-length cable introduces coupled dynamics between the load position and the cable length, since the torque exerted from the pulley affects the load position dynamics and the cable length dynamics.
- The variable length of cable introduces a Coriolis force that affects the load attitude.
- The differential flatness properties need to be re-established by using a set of flat outputs, based on the assumption $r \ll L$.

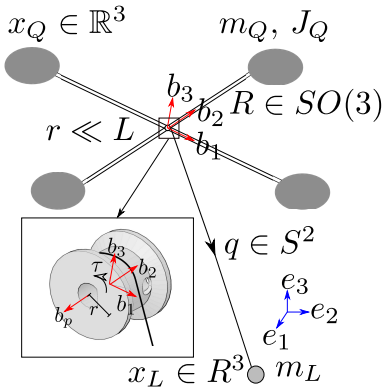

Fig. 1. Quadrotor with a cable-suspended payload with the cable length controlled by a pulley. The configuration space of the system is $SO(3) \times S^2 \times \mathbb{R} \times \mathbb{R}^3$, with 9 degrees-of-freedom and 5 actuators, resulting in 4 degrees-of-underactuation. Our control of this quadrotor-pulley-load system is designed based on the assumption that the radius of pulley is far smaller than the cable length: $r \ll L$. The simplicity and necessity of this assumption is explained in Remark 3. An inset of the pulley structure is also presented with the orientation of pulley's shaft being b_p, which is perpendicular to b_3.

However, introducing the pulley mechanism into the quadrotor-load system has advantages in path planning. Previous work on path planning for quadrotor with suspended load focused on using Mixed Integer Quadratic Programs (MIQPs) [12] or an iterative LQG (iLQG) algorithm [2] to generate collision-free quadrotor-payload trajectories. However, with a pulley mechanism we can alter the cable length to more easily avoid obstacles, instead of having the quadrotor move aggressively. This allows us to navigate tight regions such as maneuvering through windows. Moreover, the varying cable length enables payload drop off and pickup without the quadrotor having to physically move up and down, resulting in a potentially safe and energy-efficient motion.

The main contributions of this paper with respect to prior

J. Zeng, P. Kotaru and K. Sreenath are with the Dept. of Mechanical Engineering, UC Berkeley, 6141 Hearst Ave., Berkeley, CA 94720, {zengjunsjtu, prasanth.kotaru, koushils}@berkeley.edu.

This work is supported in part by NSF grant CMMI-1840219.

$\mathscr{B}$, $\mathscr{W}$	Body-fixed and world frame
$m_Q \in \mathbb{R}$	Mass of quadrotor
$m_L \in \mathbb{R}$	Mass of suspended load
$J_Q \in \mathbb{R}^{3\times3}$	Inertia matrix of the quadrotor in $\mathscr{B}$
$J_P \in \mathbb{R}$	Principal moment of inertia of pulley along b_p
$r \in \mathbb{R}$	Fixed radius of the pulley
$R \in SO(3)$	Rotation matrix from $\mathscr{B}$ to $\mathscr{W}$
$\Omega \in \mathbb{R}^3$	Angular velocity of the quadrotor in $\mathscr{B}$
$\omega \in \mathbb{R}^3$	Angular velocity of the suspended load in $\mathscr{W}$
$x_Q, v_Q \in \mathbb{R}^3$	Position and velocity vectors of the center of mass of the quadrotor in $\mathscr{W}$
$x_L, v_L \in \mathbb{R}^3$	Position and velocity vectors of the center of load of the quadrotor in $\mathscr{W}$
$f \in \mathbb{R}$	Magnitude of the thrust for the quadrotor
$M \in \mathbb{R}^3$	Moment vector for the quadrotor in $\mathscr{B}$
$\tau \in \mathbb{R}$	Pulley torque magnitude acting on pulley from quadrotor
$q \in S^2$	Unit vector from quadrotor to the load
$L \in \mathbb{R}$	Variable cable length
$e_1, e_2, e_3 \in \mathbb{R}^3$	Unit vectors along the x,y,z directions of $\mathscr{W}$
$b_1, b_2, b_3 \in \mathbb{R}^3$	Unit vectors along the x,y,z directions of $\mathscr{B}$ in $\mathscr{W}$
$e_p \in \mathbb{R}^3$	Direction of the pulley's shaft in $\mathscr{B}$
$b_p \in \mathbb{R}^3$	Direction of the pulley's shaft in $\mathscr{W}$

TABLE I

VARIOUS SYMBOLS USED IN THE PAPER

work are:

- Development of a coordinate-free dynamical model of the quadrotor-pulley-load system by applying Lagrange-d'Alembert principle and considering variations on manifolds.
- Demonstrating that the quadrotor-pulley-load system is differentially flat under the assumption $r \ll L$.
- Development of geometric controllers, along with formal proofs, for stabilizing quadrotor attitude (Prop. 1), load attitude (Prop. 2), and load position and cable length (Prop. 3).
- Numerical validation of the proposed control design to maneuver through several window-like obstacles with different sizes by dynamically varying the cable length.

The paper is organized as follows. Section II introduces the structure of the pulley and then develops a coordinate-free dynamical model for the quadrotor-pulley-load system. Section III illustrates and demonstrates the system as a differentially-flat system. Section IV presents the main ideas of the geometric controller design. Section V studies the performance of position tracking through numerical simulations. Finally, Section VI provides concluding remarks.

II. Dynamical Model of a Quadrotor-Pulley-Load System

A coordinate-free dynamic model for the quadrotor-pulley-load system is developed next. We consider the system depicted in Figure 1 with various symbols as defined in Table I. Since the cable length is controlled by a pulley placed at the center-of-mass of the quadrotor, the configuration space for the system is $Q = SO(3) \times S^2 \times \mathbb{R} \times \mathbb{R}^3$, with the degrees-of-freedom given by the quadrotor attitude $R \in SO(3)$, the unit vector $q \in S^2$ representing the load attitude, cable length $L \in \mathbb{R}$ and load position $x_L \in \mathbb{R}^3$. The system has 5 inputs comprising of the moment $M \in \mathbb{R}^3$, the thrust magnitude $f \in \mathbb{R}$ and pulley torque $\tau \in \mathbb{R}$ acting on pulley from the quadrotor.

In order to simplify our system, the pulley radius r is assumed to be constant and the direction of the shaft is assumed to be parallel to b_p in the inertia frame, with $b_p = Re_p$. The pulley shaft direction b_p can be chosen as any arbitrary unit vector orthogonal to b_3. By varying the pulley's torque, the cable can be lengthened or shortened, depending on the functional requirements of the UAV's application.

The quadrotor and load positions are related by the following geometric relation,

$$x_Q = x_L - Lq - b_p \times \frac{q - (q\cdot b_p)b_p}{||q-(q\cdot b_p)b_p||} r. \tag{1}$$

To simplify our problem, we propose an assumption $r \ll L$ which simplifies the previous kinematic relation (1) to

$$x_Q = x_L - Lq. \tag{2}$$

The necessity of this assumption will be explained in Remark 4. We next derive the coordinate-free dynamical model of the system.

The Lagrangian for the system is defined by $\mathscr{L} = \mathscr{T} - \mathscr{U}$, where $\mathscr{T}$ and $\mathscr{U}$ are kinetic and potential energies of the mechanism, respectively, and are defined as,

$$\mathscr{T} = \frac{1}{2} m_Q ||v_Q||^2 + \frac{1}{2} m_L ||v_L||^2 + \frac{1}{2} \left\langle \hat{\Omega}, \widehat{J_Q \Omega} \right\rangle + \frac{1}{2} J_P (\frac{\dot{L}}{r})^2, \tag{3}$$

$$\mathscr{U} = m_Q g e_3 \cdot x_Q + m_L g e_3 \cdot x_L. \tag{4}$$

Here, the *hat map* $\hat{\cdot} : \mathbb{R}^3 \to so(3)$ is defined as $\hat{x}y = x \times y, \forall x, y \in \mathbb{R}^3$, we also use the *vee map* $\overset{\vee}{\cdot} : so(3) \to \mathbb{R}^3$ to represent the inverse of the hat operator.

The equations of motion can then be found by using Lagrange-d'Alembert principle of least action, which states that the variation of the action integral is equal to the negative virtual work done by the external forces and non-conservative forces. The equation of Lagrange-d'Alembert principle applied to the quadrotor-pulley-load system can be written as,

$$\delta \int_{t_0}^{t_1} \mathscr{L} dt + \int_{t_0}^{t_1} \left(\left\langle W_1, \widehat{M - \tau e_p} \right\rangle + W_2 \cdot \tau + W_3 \cdot f R e_3 \right) dt = 0 \tag{5}$$

where

$$W_1 = R^T \delta R, \quad W_2 = \frac{\delta L}{r}, \quad W_3 = \delta x_Q,$$

are the variational vector fields related to quadrotor attitude, pulley rotation and quadrotor position respectively. Here, the moment vector acting on the quadrotor from the pulley is $-\tau e_p$ where τ is the torque on the pulley.

Some relations of infinitesimal variations are presented,

$$\delta R = R\hat{\eta}, \delta\Omega = \Omega\eta + \dot{\eta}, \eta \in \mathbb{R}^3,$$

$$\delta x_L = \delta x_Q + (\delta L)q + L(\delta q), (\delta x_L, \delta x_Q) \in \mathbb{R}^3, \delta L \in \mathbb{R},$$

$$\delta v_L = \delta v_Q + (\dot{\delta L})q + (\delta L)\dot{q} + \dot{L}(\delta q) + L(\dot{\delta q}),$$

$$\delta q = \xi \times q, \xi \in \mathbb{R}^3 \text{s.t.} \xi \cdot q = 0, \delta\dot{q} = \xi \times \dot{q} + \dot{\xi} \times q.$$

By solving (5), see Appendix A, we develop the dynamic model for the nonzero cable tension case.

A. Dynamical Model with Nonzero Cable Tension

The equations of motion for the quadrotor-pulley-load system are obtained as

$$\dot{x}_L = v_L, \tag{6}$$

$$\dot{q} = \omega \times q, \tag{7}$$

$$m_Q L\dot{\omega} = -q \times fRe_3 - 2m_Q\dot{L}\omega, \tag{8}$$

$$\dot{R} = R\hat{\Omega}, \tag{9}$$

$$J_Q\dot{\Omega} = M - \tau e_p - \Omega \times J_Q\Omega, \tag{10}$$

$$D\begin{bmatrix} \dot{v}_L + ge_3 \\ \ddot{L} \end{bmatrix} + H = \begin{bmatrix} (q \cdot fRe_3) \cdot q \\ \tau \end{bmatrix}, \tag{11}$$

where D and H are shown below,

$$D = \begin{bmatrix} (m_Q + m_L)I_3 & -m_Q q \\ m_L r q^T & J_P/r \end{bmatrix}, \tag{12}$$

$$H = \begin{bmatrix} m_Q L(\dot{q} \cdot \dot{q})q \\ 0 \end{bmatrix}. \tag{13}$$

Here, we have the determinant of matrix D,

$$\det(D) = \frac{1}{r}(J_p(m_Q + m_L) + m_Q m_L r^2), \tag{14}$$

is always positive which implies D can always be inverted. In the equations above, (7)-(8) ratilluste the load attitude dynamics and (9)-(10) illustrate the quadrotor attitude dynamics. Moreover, (11) illustrates the dynamic coupling between the load position and the cable length. This dynamical coupling will motivate our control design in Section IV. Note that the tension in the cable can be determined as

$$T = m_L(ge_3 + \ddot{x}_L). \tag{15}$$

Remark 1: When the tension in the cable becomes zero, the quadrotor will be decoupled from the load. In the zero-tension case, the dynamical model becomes the same as one shown in [11].

Remark 2: Note that there is no relationship between the the cable tension being zero and the pulley torque. This can be seen through the relation obtained from (11) and (15):

$$\tau = rq^T T + \frac{J_P}{r}\ddot{L}. \tag{16}$$

Therefore, even when the pulley torque becomes zero, the cable tension will be non-zero and the payload will fall slower than $-ge_3$ due to the non-zero inertia of the pulley. To make the payload free fall (zero cable tension), we need to have a positive magnitude of torque τ.

III. Differential Flatness

A system is differentially flat, if there exists a set of outputs such that the system states and the inputs can be expressed in terms of the flat output and a finite number of its derivatives. Here we will briefly present differential flatness for the quadrotor-pulley-load system.

Lemma 1: Under the assumption that the radius of the pulley is much smaller than the length of the cable $r \ll L$, the quadrotor-pulley-load system is a differentially flat system. Precisely, $Y_1 = (x_L, \psi, L)$, is a set of flat outputs for the above system, where $\psi \in \mathbb{R}$ is the yaw angle of the quadrotor.

Proof: From the flat outputs and their higher-order derivatives, the tension in the cable can be determined from (15), and the unit vector q can be determined as $q = \frac{-T}{||T||}$. Under the assumption $r \ll L$, the quadrotor position can then be determined using (2). R, Ω, f can then be determined from the knowledge of x_Q, ψ and their higher-order derivatives, since (x_Q, ψ) are flat outputs for a quadrotor as shown in [5]. From the equations of motion, the remaining M, τ can be determined from the knowledge of R, Ω, L, x_L and their higher-order derivatives. ■

Remark 3: The quadrotor moment, M, depends on the 6^{th} derivative of load position x_L and 6^{th} derivative of cable's length L, while the pulley torque depends on the 2^{nd} derivative of x_L and 2^{nd} derivative of L. This fact will be utilized for designing trajectories in Section V.

Remark 4: If we use (1) as the kinematic relation between the quadrotor and the load position the above differential flatness property is not valid anymore and (x_L, ψ, L) are no longer the flat outputs as shown next. Notice that the unit vector b_p can be calculated as $b_p = Re_p$, where R depends on the 2^{nd} derivative of x_Q as proved in [5]. This can be expressed as $b_p = h(\ddot{x}_Q)$, where $h(\cdot)$ is a function that captures this relation. If we use the full kinematic model, (1) then becomes

$$x_Q = x_L - Lq - h(\ddot{x}_Q) \times \frac{q - (q \cdot h(\ddot{x}_Q))}{||q - (q \cdot h(\ddot{x}_Q))||} r. \tag{17}$$

The quadrotor position $x_Q(t)$ can not be solved from this equation without integrating the above differential equation. Thus, to make the system become differentially flat, a simplification from (1) to (2) is necessary.

IV. Geometric Control Design

Having discussed the dynamics of the quadrotor-pulley-load system and showing that the load position and the cable's length form a set of differentially-flat outputs for the system, we now develop a controller which can be used to track one of the following states (a) quadrotor attitude in Prop.1, (b) load attitude in Prop.2, and (c) load position and cable length in Prop.3. Figure 2 illustrates the inner-outer loop controller structure for the load position and cable length tracking.

Before proceeding to describe the different controllers, we first define the configuration error for different states. Suppose a smooth desired quadrotor attitude tracking command $(R_d(t), \Omega_d(t)) \in TSO(3)$ is given. Then the real-valued configuration error function $\Psi_R : SO(3) \times SO(3) \to \mathbb{R}$ is defined as $\Psi_R = \frac{1}{2}Tr(I - R_d^T R)$, see [1]. The configuration error Ψ_R has a maximum value of 2, when R and R_d have the opposite direction, and becomes zero when $R = R_d$. Based on this notation, the vector error functions e_R and e_Ω on $T_R SO(3)$ are defined by, see [1],

$$e_R = \frac{1}{2}(R_d^T R - R^T R_d)^\vee, \qquad e_\Omega = \Omega - R^T R_d \Omega_d. \tag{18}$$

Similar to [5], the configuration error for the S^2 manifold is given as $\Psi_q = 1 - q_d^T q$, where q_d is the desired load-attitude, and vector error functions for q and $\dot{q}$ are given as follows,

$$e_q = \hat{q}^2 q_d, \qquad e_{\dot{q}} = \dot{q} - (q_d \times \dot{q}_d) \times q. \tag{19}$$

Error functions for position and velocity of the load are,

$$e_x = x_L - x_L^d, \qquad e_v = v_L - v_L^d, \tag{20}$$

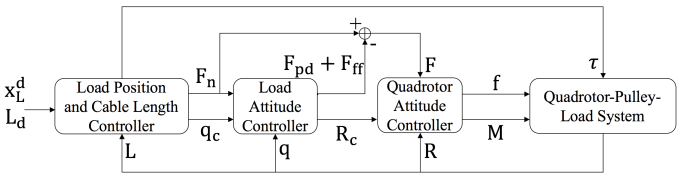

Fig. 2. Controller structure for tracking load position. Notice that the desired values are calculated in the inner loop controller, such as q_c and R_c, while the actual states are feedback for each part of the controllers, for example, L, q, R. The calculated outputs for the system are M, τ and f.

where x_L^d and v_L^d are the desired position and velocity of the load. Error function for cable length is defined as,

$$e_L = L - L_d, \tag{21}$$

where $L_d(t)$ is the desired cable length as a function of time. Higher order error are also defined as follow,

$$\dot{e}_L = \dot{L} - \dot{L}_d, \qquad \ddot{e}_L = \ddot{L} - \ddot{L}_d. \tag{22}$$

Proposition 1: (Almost Global Exponential Stability of Quadrotor Attitude Controlled Flight Mode)

Consider the quadrotor dynamical model in (9)-(10). We introduce a nonlinear controller for the attitude controlled flight mode, described by an expression for the moment vector:

$$\begin{aligned} M = &-\frac{k_R}{\varepsilon^2}e_R - \frac{k_\Omega}{\varepsilon}e_\Omega + \Omega \times J_Q\Omega \\ &- J_Q(\hat{\Omega}R^T R_d\Omega_d - R^T R_d\dot{\Omega}_d) + \tau e_p, \end{aligned} \tag{23}$$

for any positive constants k_R, k_ω and $0 < \varepsilon < 1$.

Further, suppose the initial condition satisfies

$$\Psi_R(R(0), R_d(0)) < 2, \tag{24}$$

$$||e_\Omega||^2 < \frac{2}{\lambda_M(J_Q)}\frac{k_R}{\varepsilon^2}(2 - \Psi_R(R(0), R_d(0))). \tag{25}$$

In this case, the zero equilibrium of the closed loop tracking error $(e_R, e_\Omega) = (0,0)$ is exponentially stable. Furthermore, there exist constants α_R, $\beta_R > 0$ such that,

$$\Psi_R(R(t), R_d(t)) \leq min\{2, \alpha_R e^{-\beta_R t}\}. \tag{26}$$

Remark 5: The controller (23) is a geometric version of PD control along with a feedforward term. We have an additional term τe_p which represents the additional moment compensating the moment on the quadrotor from pulley shown in (10).

Proof: With the exception of the additional torque τe_p, the control design is from [11, Prop. 1] by defining $k_R^\varepsilon = \frac{k_R}{\varepsilon^2}$, $k_\Omega^\varepsilon = \frac{k_\Omega}{\varepsilon^2}$. The parameter ε is introduced to enable rapid exponential convergence. ■

Proposition 2: (Almost Global Exponential Stability of Load Attitude Controlled Flight Mode) Consider the load attitude dynamics given by (7)-(8) along with the quadrotor attitude dynamics (9)-(10), and consider the desired quadrotor attitude as,

$$R_c := [b_{1c}; b_{3c} \times b_{1c}; b_{3c}], \quad \hat{\Omega}_c = R_c^T\dot{R}_c, \tag{27}$$

where $b_{3c} \in S^2$ is defined by

$$b_{3c} = \frac{F}{||F||}, \tag{28}$$

$$F = F_n - F_{pd} - F_{ff}, \tag{29}$$

where F_n, F_{pd}, F_{ff} are defined respectively as

$$F_n = -(q_d \cdot q)\cdot q, \tag{30}$$

$$F_{pd} = -k_q e_q - k_{\dot{q}} e_{\dot{q}}, \tag{31}$$

$$F_{ff} = m_Q L\langle q, \omega_d\rangle\,\omega + m_Q L\dot{\omega}_d \times q + 2m_Q\dot{L}(\omega \times q), \tag{32}$$

where ω_d represents the desired angular velocity of load attitude. We choose $b_{1d} \in S^2$ not parallel to b_{3c} and define

$$b_{1c} = -\frac{1}{||b_{3c} \times b_{1d}||}(b_{3c} \times (b_{3c} \times b_{1d})), \tag{33}$$

and the quadrotor thrust is computed as,

$$f = F \cdot R\mathbf{e}_3, \tag{34}$$

with the quadrotor moment defined by (23) with the computed values, R_c , Ω_c used instead of the the desired ones. Suppose the initial conditions satisfy

$$\Psi_q(q(0), q_d(0)) < 2, \tag{35}$$

$$||e_{\dot{q}}(0)||^2 < \frac{2}{m_Q L}k_q(2 - \Psi_q(q(0), q_d(0))), \tag{36}$$

then there exists $\bar{\varepsilon}_q$, such that for all $0 < \varepsilon < \bar{\varepsilon}_q$, the zero equilibrium of the closed loop tracking error $(e_q, e_{\dot{q}}, e_R, e_\Omega) = (0,0,0,0)$ is exponentially stable. Furthermore, there exist constants $\alpha_q, \beta_q > 0$ such that,

$$\Psi_q(q(t), q_d(t)) < min\{2, \alpha_q e^{-\beta_q t}\}. \tag{37}$$

The domain of attraction is characterized by (24), (25), (35), (36). Moreover, the region of the state space $TS^2 \times TSO(3)$ that does not converge to the equilibrium is of measure zero, resulting in almost global exponential stability.

Proof: A very similar control design can be found [11, Prop. 2] and the only difference between our controller and the one in [11, Prop.2] is specified in (32), where the term $2m_Q\dot{L}(\omega \times q)$ is added to compensate the Coriolis force in (8) that is due to the variable-length cable. Note that this proof of stability is based on the slow model (model without quadrotor attitude dynamics) [1, Lemma 11.23] and established through a singular perturbation argument (Tychnoff Theorem) [3, Thm. 11.2]. ■

Proposition 3: (Exponential Stability of Load Position and Cable Length Controlled Flight Mode) Considering the coupled dynamics in (11), we introduce a PD controller for the the load position and cable length controlled flight mode, described by two expressions for A and τ

$$\begin{bmatrix} A \\ \tau \end{bmatrix} = D\begin{bmatrix} \dot{v}_L^d + ge_3 - k_x e_x - k_v e_v \\ \ddot{L}_d - k_L e_L - k_{\dot{L}}\dot{e}_L \end{bmatrix} + H, \tag{38}$$

where k_x, k_v, k_L, $k_{\dot{L}}$ are strictly postive and the computed load attitude is,

$$q_c = -\frac{A}{||A||}, \tag{39}$$

and we assume that $||A|| \neq 0$ and the commanded acceleration is uniformly bounded such that,

$$||D_{11}(\dot{v}_L^d + ge_3) + D_{12}\ddot{L}^d + m_Q L(\dot{q}\cdot\dot{q})q|| \leq B, \tag{40}$$

where D_{ij} are the i^{th} row j^{th} column submatrices of D in (12). Furthermore, define F_n in (30) as

$$F_n = (A \cdot q)\cdot q. \tag{41}$$

Let the computed quadrotor attitude be defined by (27), (28), with the quadrotor thrust and moment defined by (23) and (34), with the desired quadrotor and load attitude replaced by their computed values, R_c and q_c respectively. Further,

suppose the initial conditions of load attitude, load position and cable length satisfy

$$\Psi_q(q(0),q_c(0)) < \psi_1 < 1, \tag{42}$$

$$||e_x(0)|| < e_{x_{max}}, \quad ||e_v(0)|| < e_{v_{max}}, \tag{43}$$

$$|e_L(0)| < e_{L_{max}}, \quad |\dot{e}_L(0)| < |e_{\dot{L}_{max}}|, \tag{44}$$

for a fixed constant $e_{x_{max}}$, $e_{v_{max}}$, $e_{L_{max}}$, $e_{\dot{L}_{max}}$ and ψ_1. We introduce positive constants k'_x, k'_v, k'_L, $k'_{\dot{L}}$ and B',

$$\begin{aligned} \frac{k'_x}{k_x} = \frac{k'_v}{k_v} &= \left\| D^{-1} \begin{bmatrix} D_{11} \\ 0 \end{bmatrix} \right\|_2 < 1, \\ \frac{k'_L}{k_L} = \frac{k'_{\dot{L}}}{k_{\dot{L}}} &= \left\| D^{-1} \begin{bmatrix} D_{12} \\ 0 \end{bmatrix} \right\|_2 < 1, \end{aligned} \tag{45}$$

where the boundedness of (45) can be verified by using the positiveness of det(D). According to the uniform boundedness in (40), $B' \in \mathbb{R}$ is defined to satisfy

$$B' = \left\| D^{-1} \begin{bmatrix} I_3 \\ 0 \end{bmatrix} \right\|_2. \tag{46}$$

Define $W_L, W_x \in \mathbb{R}^{2\times 2}$ and $W_{lq}, W_{xq} \in \mathbb{R}^2$ as,

$$W_x = \begin{bmatrix} c_1(k_x - k'_x\alpha) & -\frac{1}{2}c_1(k_v + k'_v) \\ -\frac{1}{2}c_1(k_v + k'_v) & k_v - k'_v - c_1 \end{bmatrix}, \tag{47}$$

$$W_{xq} = \begin{bmatrix} c_1 B' \\ k'_x e_{xmax} + B' \end{bmatrix}, \tag{48}$$

$$W_{Lq} = \begin{bmatrix} c_2 B' \\ k'_L e_{Lmax} + B' \end{bmatrix}, \tag{49}$$

$$W_L = \begin{bmatrix} c_2(k_L - k'_L\alpha) & -\frac{1}{2}c_2(k_{\dot{L}} + k'_{\dot{L}}) \\ -\frac{1}{2}c_2(k_{\dot{L}} + k'_{\dot{L}}) & k_{\dot{L}} - k'_{\dot{L}} - c_2 \end{bmatrix}, \tag{50}$$

where $\alpha := \sqrt{\psi_1(2-\psi_1)}$, and c_1, c_2 are positive constant such that,

$$c_1 < \min\left\{ k_v - k'_v\alpha, \sqrt{k_x}, \frac{4(k_x - k'_x\alpha)(k_v - k'_v\alpha)}{(k_v + k'_v)^2 + 4(k_x - k'_x\alpha)} \right\}, \tag{51}$$

$$c_2 < \min\left\{ k_{\dot{L}} - k'_{\dot{L}}\alpha, \sqrt{k_L}, \frac{4(k_L - k'_L\alpha)(k_{\dot{L}} - k'_{\dot{L}}\alpha)}{(k_{\dot{L}} + k'_{\dot{L}})^2 + 4(k_L - k'_L\alpha)} \right\}, \tag{52}$$

$$\lambda_m(W_q) > \max\left\{ \frac{||W_{Lq}||^2}{2\lambda_m(W_L)}, \frac{||W_{xq}||^2}{2\lambda_m(W_x)} \right\}. \tag{53}$$

Then, there exists $\bar{\varepsilon}_x$, such that for all $0 < \varepsilon < \bar{\varepsilon}_x$, the zero equilibrium of the closed loop tracking error $(e_L, e_{\dot{L}}, e_x, e_v, e_q, e_{\dot{q}}, e_R, e_\Omega) = (0,0,0,0,0,0,0,0)$ is exponentially stable. The domain of attraction is characterized by (35), (36) with the desired values replaced by the computed values, (42), and

$$||e_{\dot{q}}|| < \frac{2}{m_Q l} k_q (\psi_1 - \Psi_q(q(0), q_d(0))). \tag{54}$$

Proof: This proposition is motivated by [11, Prop. 3] which was proving exponential stability of the quadrotor-load system through a singular perturbation argument. Here we address the quadrotor-pulley-load system, where another degree-of-freedom for the variable-length cable is added. See detailed proof in Appendix B. ■

V. Numerical Simulation

Having developed the geometric dynamics and control of the quadrotor-pulley-load system with the additional degree-of-freedom for cable length, we can do path planning and control in more complex environments. In particular, we consider manipulating the quadrotor-pulley-load system to pass through window-like obstacles with different heights, a common scenario to test path planning for obstacle avoidance [2], [12]. The window height can be chosen to be smaller than the cable's initial length, forcing the quadrotor to pull up the load by decreasing the cable length to allow it to pass through the windows.

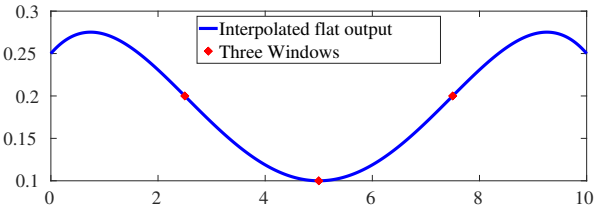

Fig. 3. Evolution of desired cable length (blue) required to pass three given windows during 10 seconds. Note that the desired cable length when passing the windows (red) is exactly one third of window's height to ensure safety.

Since the quadrotor-pulley-load system is differentially flat under the assumption $r \ll L$, we can plan and study trajectories directly in the flat space. We do this by parametrizing the flat outputs as functions of time with a suitable basis and solve an optimization problem to obtain the coefficients of the basis. To illustrate our performance, we aim to manipulate the quadrotor to adjust its cable length to pass through three windows by tracking a specific trajectory. The positions (X_i), widths (W_i) and heights (H_i) of the three windows are given below,

$$\begin{aligned} X_1 = (A_x, A_y, A_z + Z_0), \quad W_1 = 0.4m, \quad H_1 = 0.6m, \\ X_2 = (2A_x, 0, Z_0), \quad W_2 = 0.4m, \quad H_2 = 0.3m, \\ X_3 = (A_x, -A_y, -A_z + Z_0), \quad W_3 = 0.4m, \quad H_3 = 0.6m. \end{aligned}$$

In consideration of passing through the three windows, we choose the flat outputs as follows.

$$x_L^d(t) = \left[A_x(1 - cos(\frac{2\pi t}{T})), A_y sin(\frac{2\pi t}{T}), A_z sin(\frac{2\pi t}{T}) + Z_0 \right]^T, \tag{55}$$

$$\psi_d(t) \equiv 0, \tag{56}$$

where T is the time period of the circular orbit of the load trajectory. Numerically we choose $T = 10s$, $A_x = 3m$, $A_y = 3m$ and $A_z = 2m$.

In order to maneuver through these obstacles, we need to specify different desired cable length for each pass. Here we choose $0.2m$, $0.1m$, $0.2m$ respectively, which are one third of each window's height. As the function $L_d(t)$ needs to be high-order differentiable according to Remark 2, one choice of flat outputs of cable length is given as follows, illustrated in Figure 3,

$$L_d(t) = -\frac{1}{1875}t^4 + \frac{4}{375}t^3 - \frac{91}{1500}t^2 + \frac{11}{150}t + \frac{1}{4}. \tag{57}$$

This expression of desired cable length is calculated by interpolation from the Polynomial Toolbox in Matlab, such that it satisfies the desired cable lengths when passing through each window. While we used a polynomial basis here, other basis such as sinusoidal basis can also be used.

We consider a realistic experimental platform with $m_Q = 0.5kg$, $m_L = 0.087kg$, $J_Q = diag(2.32, 2.32, 4) \times 10^{-3} kg \cdot m^3$, $J_P = 3 \times 10^{-4} kg \cdot m^3$ and $r = 0.03m$. We also assume that the thrust and the moment of quadrotor are bounded, with $|f| \leq 10N$ and $||M|| \leq 2N \cdot m$.

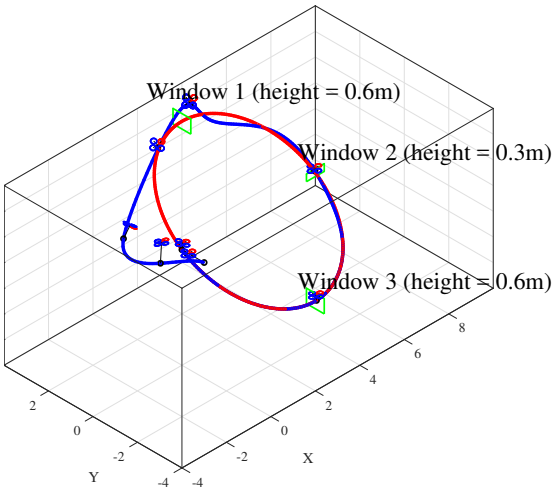

Fig. 4. Snapshots of the quadrotor along the executed motion (blue) as it tracks the desired load position (red). Notice the large initial errors in load position and cable length. The initial cable length is 1m with the cable length varying to pass through the windows.

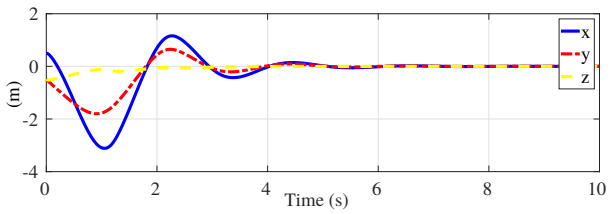

Fig. 5. Error in load position tracking. Notice that the position error in direction z is rejected more quickly than the other directions.

We present a simulation with the initial condition specifying errors in load attitude, load position and cable length. Specifically, the initial cable length is 1m and there is about 1m initial load position error and the load attitude is released from 45°. A desired time-varying load position trajectory, yaw angle and cable length are shown in (55)-(57) and the system is simulated with the controller in Proposition 3. Figure 4 illustrates the trajectory of the load as it converges to the desired load position trajectory as well as snapshots of the quadrotor when passing through windows. Figures 5, 6 illustrate the load position and cable length error, while Figure 7 illustrates the configuration error for the quadrotor and the load attitude. Note that the double peaks in Ψ_q occur due to the controller implementation of using the nominal desired quantities $\dot{R}_d$, $\ddot{R}_d$, $\dot{q}_d$, $\ddot{q}_d$ from differential flatness instead of the computed values $\dot{R}_c$, $\ddot{R}_c$, $\dot{q}_c$ and $\ddot{q}_c$. The computed inputs are shown in Figure 8.

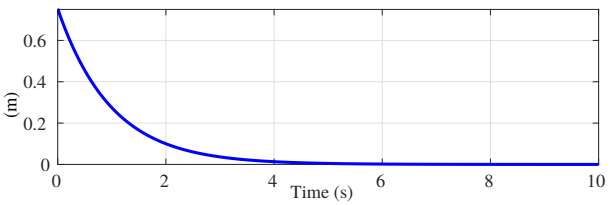

Fig. 6. Error in cable length tracking exponentially decaying to zero.

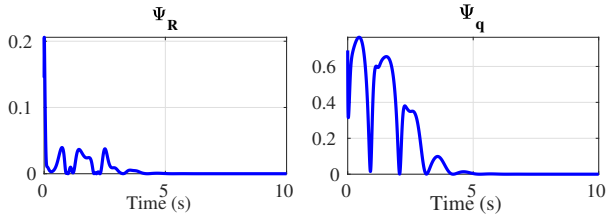

Fig. 7. Configuration error functions for the quadrotor attitude and the load attitude. In this simulation, the controller rejects initial attitude errors of 45° in both the quadrotor and load attitudes.

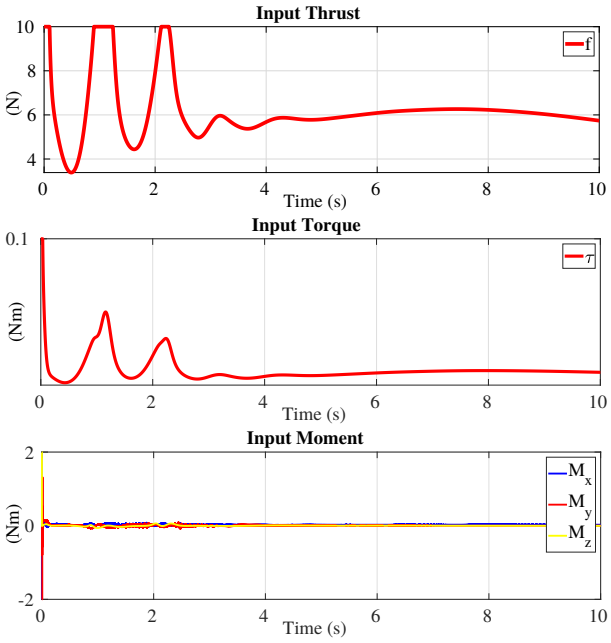

Fig. 8. Inputs for the load tracking of the trajectory shown in Figure 4. We observe that the errors decay exponentially even with a saturated thrust f and moment M.

VI. Conclusion

We have presented a coordinate-free development of the dynamics of a quadrotor with a variable length cable-suspended load, where the cable length can be changed by varying the torque on a pulley attached to the quadrotor. The differential flatness of the quadrotor-pulley-load system is shown based on the assumption $r \ll L$ and has been utilized to design nominal trajectories. A nonlinear geometric control design was presented that enabled tracking of either the quadrotor attitude, the load attitude, or the load position and the cable length. The stability of the proposed controllers were formally proved and the controllers were numerically validated through a concrete scenario of passing through windows with different heights.

Appendix

A. Derivation of the dynamics for the quadrotor-pulley-load system

In this section we present the detailed derivation of the compact equations of motion on manifolds for the quadrotor-

pulley-load system.

$$\delta \int_{t_0}^{t_1} (\frac{1}{2} m_Q v_Q \cdot v_Q + \frac{1}{2} m_L v_L \cdot v_L + \frac{1}{2} \langle \Omega, J_Q \Omega \rangle + \frac{1}{2} J_P (\frac{\dot{L}}{r})^2 - m_Q g e_3 \cdot x_Q - m_L g e_3 \cdot x_L) dt + \int_{t_0}^{t_1} \Big(\langle R^T \delta R, \widehat{M - \tau e_p} \rangle + \frac{\delta L}{r} \cdot \tau + (\delta x_L - \delta L \cdot q - L \delta q) \cdot f R e_3 \Big) dt = 0$$

By using the relations of infinitesimal variations to substitute the terms of δx_Q, $\delta \dot{x}_Q$, $\delta \ddot{x}_Q$, we have,

$$\begin{aligned}
&\int_{t_0}^{t_1} \delta \dot{x}_L \cdot \big[m_Q (v_L - \dot{L} q - L \dot{q}) + m_L v_L \big] + \delta x_L \cdot (-m_Q g e_3 - m_L g e_3 + f R e_3) dt \\
&+ \int_{t_0}^{t_1} \delta \dot{L} \cdot \big[- m_Q q (\dot{x}_L - \dot{L} q - L \dot{q}) + \frac{J_P \dot{L}}{r^2} \big] + \delta L \cdot \big[\\
&\quad - m_Q \dot{q} (\dot{v}_L - \dot{L} q - L \dot{q}) + m_Q g q e_3 + \frac{\tau}{r} - q \cdot f R e_3 \big] dt \\
&+ \int_{t_0}^{t_1} \delta \dot{q} \cdot \big[- m_Q (v_L - \dot{L} q - L \dot{q}) L \big] \\
&\quad + \delta q \cdot \big[- m_Q (v_L - \dot{L} q - L \dot{q}) \dot{L} + m_Q g L e_3 - L f R e_3 \big] dt \\
&+ \int_{t_0}^{t_1} \big[\dot{\eta} J \Omega + \eta (M - \tau e_p + J_Q \Omega \times \Omega) \big] dt = 0
\end{aligned}$$

Then we apply the integrations by parts and the dynamical system derived by the Lagrange-d'Alembert principle can be written as,

$$\begin{aligned}
&\int_{t_0}^{t_1} \Big(\delta x_L \cdot \big[- (m_Q + m_L)(\dot{v}_L + g e_3) \\
&\quad + m_Q (\ddot{L} q + 2 \dot{L} \dot{q} + L \ddot{q}) + f R e_3 \big] \Big) dt \\
&+ \int_{t_0}^{t_1} \Big(\delta L \cdot \big[- m_Q q (\ddot{L} q + 2 \dot{L} \dot{q} + L \ddot{q}) \\
&\quad + m_Q q (\dot{v}_L + g e_3) - \frac{J_P \ddot{L}}{r^2} + \frac{\tau}{r} - q \cdot f R e_3 \big] \Big) dt \qquad (58) \\
&+ \int_{t_0}^{t_1} \Big(\xi \cdot \big[q \times m_Q L (\dot{v}_L - \ddot{L} q - 2 \dot{L} \dot{q} \\
&\quad - L \ddot{q}) + q \times (m_Q g L e_3 - L f R e_3) \big] \Big) \\
&+ \int_{t_0}^{t_1} \Big(\eta \cdot \big[- J \dot{\Omega} - \Omega \times J \Omega + M - \tau e_p \big] \Big) dt = 0.
\end{aligned}$$

Since (58) is always true for all variations δx_L, δL, $\delta \xi$ and $\delta \eta$, we have,

$$(m_Q + m_L)(\dot{v}_L + g e_3) = m_Q (\ddot{L} q + 2 \dot{L} \dot{q} + L \ddot{q}) + f R e_3, \qquad (59)$$

$$- m_Q q (\ddot{L} q + 2 \dot{L} \dot{q} + L \ddot{q}) + m_Q q (\dot{v}_L + g e_3) - \frac{J_P \ddot{L}}{r^2} + \frac{\tau}{r} = q \cdot f R e_3, \qquad (60)$$

$$q \times [q \times m_Q L (\dot{v}_L - \ddot{L} q - 2 \dot{L} \dot{q} - L \ddot{q}) + q \times (m_Q g L e_3 - L f R e_3)] = 0, \qquad (61)$$

$$- J \dot{\Omega} - \Omega \times J \Omega + M - \tau e_p = 0. \qquad (62)$$

Simplifying these equations results in the equations of motion given in (8), (10), (11).

B. Proof for Proposition 3

We will consider the slow model and carry out the subsequent analysis in the domain $\mathscr{D}$,

$$\mathscr{D} = \{ (e_L, \dot{e}_L, e_x, e_v, q, e_{\dot{q}}) \in \mathbb{R} \times \mathbb{R} \times \mathbb{R}^3 \times \mathbb{R}^3 \times L_1 \times \mathbb{R}^3 \mid |e_L| < e_{L_{max}}, ||e_x|| < e_{x_{max}} \} \qquad (63)$$

where the load attitude is restricted to be in the sublevel set $L_1 = \{ q \in S^2 \mid \Psi_q(q, q_c) < 1 \}$.

1) Translational and Cable Length Error Dynamics for Slow Model: Similar to [11, Appendix B], we introduce $X \in \mathbb{R}^3$, representing the error between $(q \cdot f R e_3) q$ and $\frac{(q \cdot f R e_3) q_c}{q_c^T q}$, defined by,

$$X = \frac{q \cdot f R e_3}{q_c^T q} ((q_c \cdot q) q - q_c), \qquad (64)$$

where we have

$$\begin{aligned}
q \cdot f R e_3 &= q \cdot F = q \cdot (F_n - F_{pd} - F_{ff}) \\
&= A \cdot q = - ||A|| q_c \cdot q.
\end{aligned} \qquad (65)$$

Then, $||X||$ is bounded by the multiplication between the norms of A and the error of load attitude e_q,

$$||X|| \leq ||A|| \cdot ||((q_c \cdot q) q - q_c)||. \qquad (66)$$

Substituting (64) into (11), we have

$$\begin{bmatrix} A + X \\ \tau \end{bmatrix} = D \begin{bmatrix} \dot{v}_L + g e_3 \\ \ddot{L} \end{bmatrix} + H. \qquad (67)$$

In addition to the controller defined in (38), the translational and cable length error dynamics can be written as,

$$\begin{bmatrix} \dot{e}_v \\ \ddot{e}_L \end{bmatrix} = \begin{bmatrix} -k_x e_x - k_v e_v \\ -k_L e_L - k_{\dot{L}} \dot{e}_L \end{bmatrix} + D^{-1} \begin{bmatrix} X \\ 0 \end{bmatrix}. \qquad (68)$$

Considering the coupled controller presented in (38),

$$\begin{aligned}
||A|| =& ||[D_{11} (\dot{v}_L^d + g e_3) + D_{12} \ddot{L}^d + m_Q L (\dot{q} \cdot \dot{q}) q] \\
&- D_{11} (k_x e_x + k_v e_v) - D_{12} (k_L e_L + k_{\dot{L}} \dot{e}_L)|| \\
\leq& B + ||D_{11}||_2 (k_x ||e_x|| + k_v ||e_v||) + |D_{12}| (k_L |e_L| + k_{\dot{L}} |\dot{e}_L|).
\end{aligned}$$

The bound of $||X||$ can then be found by substituting the above bound on $||A||$ into (66), resulting in,

$$\begin{aligned}
||X|| \leq& (B + ||D_{11}||_2 (k_x ||e_x|| + k_v ||e_v||) \\
&+ |D_{12}| (k_L |e_L| + k_{\dot{L}} |\dot{e}_L|)) ||e_q||.
\end{aligned} \qquad (69)$$

Thus, the translational and cable length error dynamics in (68) can be simplified by substituting (69) into (68).

$$\begin{bmatrix} \dot{e}_v \\ \ddot{e}_L \end{bmatrix} = \begin{bmatrix} -k_x e_x - k_v e_v + X_1 \\ -k_L e_L - k_{\dot{L}} \dot{e}_L + X_2 \end{bmatrix}, \qquad (70)$$

where $X_1 \in \mathbb{R}^3$ and $X_2 \in \mathbb{R}$ are defined as $\begin{bmatrix} X_1 \\ X_2 \end{bmatrix} = D^{-1} \begin{bmatrix} X \\ 0 \end{bmatrix}$, satisfying

$$\begin{aligned}
||X_1|| &\leq (B' + k_x' ||e_x|| + k_v e_v) ||e_q||, \\
|X_2| &\leq (B' + k_L' |e_L| + k_{\dot{L}}' |\dot{e}_L|) ||e_q||,
\end{aligned} \qquad (71)$$

where $k_x', k_v', k_L', k_{\dot{L}}', B'$ are defined in (45) and (46). In the following subsection, we define a Lyapunov Candidate for the error dynamics along the solution in (70).

2) Lyapunov Candidate for Translation Dynamics: Consider the Lyapunov candidate V_x,

$$V_x = \frac{1}{2} k_x ||e_x||^2 + \frac{1}{2} ||e_v||^2 + c_1 e_x e_v, \qquad (72)$$

where c_1 is a positive constant. The derivative of V_x along the solution of (70) is given by

$$\begin{aligned}
\dot{V}_x =& k_x e_x \cdot e_v + e_v \cdot (-k_x e_x - k_v e_v + X_1) + c_1 e_v \cdot e_v \\
&+ c_1 e_x (-k_x e_x - k_v e_v + X_1) - c_1 k_x e_x^2 \\
&- (k_v - c_1) e_v^2 - c_1 k_v e_x e_v + X_1 (e_v + c_1 e_x).
\end{aligned}$$

Since the bound of $||X_1||$ is represented in (71), thus we have,

$$\begin{aligned}
\dot{V}_x \leq& - c_1 k_x e_x^2 - (k_v - c_1) e_v^2 - c_1 k_v e_x e_v \\
&+ (k_x' ||e_x|| + k_v' ||e_v|| + B') ||e_q|| (e_v + c_1 e_x) \\
\leq& - c_1 (k_x - k_x' \alpha) e_x^2 - (k_v - c_1 - k_v' \alpha) e_v^2 + c_1 (k_v + \\
&k_v') ||e_x e_v|| + ||e_q|| \{ k_x' ||e_x|| ||e_v|| + c_1 B' ||e_x|| + B' ||e_v|| \}.
\end{aligned} \qquad (73)$$

In the above expression, there is a third-order term, $k_x' ||e_x|| ||e_v|| ||e_q||$. Since we restrict our analysis to the domain $\mathscr{D}$ defined in (63), an upper bound for this term is $k_x' e_{xmax} ||e_v|| ||e_q||$.

3) Lyapunov Candidate for Cable Length Dynamics: Similarly, consider the Lyapunov candidate V_L,

$$V_L = \frac{1}{2}k_L|e_L|^2 + \frac{1}{2}|\dot{e}_L|^2 + c_2 e_L \dot{e}_L, \tag{74}$$

where c_1 is a positive constant. The derivative of V_x along the solution of (70) is given by

$$\begin{aligned}\dot{V}_L =& k_L e_L \cdot \dot{e}_L + \dot{e}_L \cdot (-k_L e_L - k_{\dot{L}} \dot{e}_L + X_2) + c_2 \dot{e}_L \cdot \dot{e}_L \\ &+ c_2 e_L(-k_L e_L - k_{\dot{L}} \dot{e}_L + X_2) - c_2 k_L e_L^2 \\ &- (k_{\dot{L}} - c_2)\dot{e}_L^2 - c_2 k_{\dot{L}} e_L \dot{e}_L + X_2(\dot{e}_L + c_2 e_L).\end{aligned}$$

Since the bound of $|X_2|$ is represented in (71), thus we have,

$$\begin{aligned}\dot{V}_L \leq& -c_2 k_L e_L^2 - (k_{\dot{L}} - c_2)\dot{e}_L^2 - c_2 k_{\dot{L}} e_L \dot{e}_L \\ &+ (k'_L|e_L| + k'_{\dot{L}}|\dot{e}_L| + B')||e_q||(\dot{e}_L + c_2 e_L) \\ \leq& -c_2(k_L - k'_L\alpha)e_L^2 - (k_{\dot{L}} - c_2 - k'_{\dot{L}}\alpha)\dot{e}_L^2 + c_2(k_{\dot{L}} + \\ &k'_{\dot{L}})|e_L \dot{e}_L| + ||e_q||\{k'_L|e_L||\dot{e}_L| + c_2 B'|e_L| + B'|\dot{e}_L|\}.\end{aligned} \tag{75}$$

In the above expression, there is a third-order term, $k'_L|e_L||\dot{e}_L|||e_q||$. Since we restrict our analysis to the domain $\mathscr{D}$ defined in (63), an upper bound for this term is $k'_L e_{Lmax}|\dot{e}_L|||e_q||$.

4) Lyapunov Candidate for the Slow Model: Let $V = V_x + V_q + V_L$ be the Lyapunov candidate for the slow model and the expression of V_q can be found [11, Appendix A]. Then, from (72), (73), (74), (75), we have,

$$z_x^T M_x z_x + z_q^T M_q z_q + z_L^T M_l z_L \leq V \leq z_x^T M_X z_x + z_q^T M_Q z_q + z_L^T M_L z_L,$$

$$\dot{V} \leq -z_x^T W_x z_x + z_x^T W_{xq} z_q - z_L^T W_L z_L + z_L^T W_{Lq} z_q - z_q^T W_q z_q,$$

where $z_x = [||e_x||, ||e_v||]^T$, $z_L = [|e_L|, |\dot{e}_L|]^T$, and the matrices W_x, W_{xq}, W_L, W_{Lq} are as in (47), (48), (50), (49), while M_x, M_X, M_l, M_L are defined as

$$M_x = \frac{1}{2}\begin{bmatrix} k_x & -c_1 \\ -c_1 & 1 \end{bmatrix}, M_X = \frac{1}{2}\begin{bmatrix} k_x & c_1 \\ c_1 & 1 \end{bmatrix}, \tag{76}$$

$$M_l = \frac{1}{2}\begin{bmatrix} k_L & -c_2 \\ -c_2 & 1 \end{bmatrix}, M_L = \frac{1}{2}\begin{bmatrix} k_L & c_2 \\ c_2 & 1 \end{bmatrix}. \tag{77}$$

5) Exponential Stability: From [11, Proposition 2], the matrices M_q, M_Q, W_q are positive definite, while (51), (52) ensure positive-definiteness of M_x, M_X, M_l, M_L. Then the candidate Lyapunov function V is positive-definite, and

$$\begin{aligned}\dot{V} \leq& -\lambda_m(W_L)||z_L||^2 + ||W_{Lq}||_2||z_L||||z_q|| - \lambda_m(W_q)||z_q||^2 \\ &- \lambda_m(W_x)||z_x||^2 + ||W_{xq}||_2||z_x||||z_q||.\end{aligned} \tag{78}$$

The conditions of Proposition 3, (51), (52) ensures positive-definiteness of W_x and W_L and (53) for negative-definiteness of $\dot{V}$.

Thus the zero equilibrium of the load position tracking errors of the slow model is exponentially stable, i.e., $(e_x, e_v, e_L, \dot{e}_L, e_q, e_{\dot{q}})$ exponentially converges to zero while the dynamics evolve on the slow manifold given by $R \equiv R_c$. We employ the singular perturbation argument again, which results in exponential stability of load position and cable length dynamics for the full model, see [11, Prop. 4].

REFERENCES

[1] F. Bullo and A. D. Lewis, *Geometric Control of Mechanical Systems*. New York-Heidelberg-Berlin: Springer-Verlag, 2004.

[2] C. de Crousaz, F. Farshidian, and J. Buchli, "Aggressive optimal control for agile flight with a slung load," in *"IEEE Int. Conf. on Intelligent Robots and Systems"*, 2014.

[3] H. K. Khalil, *Nonlinear Control*. New Jersey: Prentice Hall, 2002.

[4] P. Kotaru, G. Wu, and K. Sreenath, "Dynamics and control of a quadrotor with a payload suspended through an elastic cable," in *IEEE American Control Conference*, 2017, pp. 3906–3913.

[5] T. Lee, M. Leok, and N. H. McClamroch, "Control of complex maneuvers for a quadrotor uav using geometric methods on se(3)," in *IEEE Int. Conf. on Decision and Control*, 2010, pp. 5420–5425.

[6] T. Lee, K. Sreenath, and V. Kumar, "Geometric control of cooperating multiple quadrotor uavs with a suspended payload," in *IEEE Int. Conf. on Decision and Control*, 2013, pp. 5510–5515.

[7] D. Mellinger, Q. Lindsey, M. Shomin, and V. Kumar, "Design, modeling, estimation and control for aerial grasping and manipulation," in *IEEE Int. Conf. on Intelligent Robots and Systems*, 2011, pp. 2668–2673.

[8] D. Mellinger, Q. Lindsey, M. Shominand, and V. Kumar, "Trajectory generation for swing-free maneuvers of a quadrotor with suspended payload: A dynamic programming approach," in *IEEE Int. Conf. on Robotics and Automation*, 2012, pp. 2668–2673.

[9] I. Palunko, A. Faust, P. Cruz, L. Tapia, and R. Fierro, "A reinforcement learning approach towards autonomous suspended load manipulation using aerial robots," in *IEEE Int. Conf. on Robotics and Automation*, 2013, pp. 4896–4901.

[10] K. Sreenath and V. Kumar, "Dynamics, control and planning for cooperative manipulation of payloads suspended by cables from multiple quadrotor robots," in *Robotics: Science and Systems (RSS)*, 2013.

[11] K. Sreenath, T. Lee, and V. Kumar, "Geometric control and differential flatness of a quadrotor uav with a cable-suspended load," in *IEEE Int. Conf. on Decision and Control*, 2013, pp. 2269–2274.

[12] S. Tang and V. Kumar, "Mixed integer quadratic program trajectory generation for a quadrotor with a cable-suspended payload," in *IEEE Int. Conf. on Robotics and Automation*, 2015, pp. 2216–2222.

[13] S. Tang, V. Wüest, and V. Kumar, "Aggressive flight with suspended payloads using vision-based control," *IEEE Robotics and Automation Letters*, vol. 3, no. 2, pp. 1152–1159, 2018.

[14] G. Wu and K. Sreenath, "Geometric control of multiple quadrotors transporting a rigid-body load," in *IEEE International Conference on Decision and Control*, 2014, pp. 6141–6148.